

Available online at www.sciencedirect.com

ScienceDirect

journal homepage: www.elsevier.com/locate/he

A novel method for industrial production of clean hydrogen (H₂) from mixed plastic waste

Patient E. Ganza ^{a,b}, BongJu Lee ^{a,b,*}

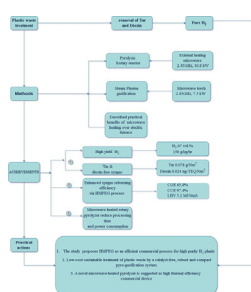
^a Department of Computer Science and Electrical Engineering, Handong Global University, Pohang 791-708, S. Korea

^b Green Science Co, South Korea

HIGHLIGHTS

- The efficiency of producing H₂ stands at 67% and syngas reforming efficiency is 65.8%.
- Hybrid process minimizes bio-oils by converting the maximum tar content in pyro-gas.
- The plasma torch allows the complete removal of dioxin and other toxic byproducts.
- We propose a novel rotary microwave-heated pyrolyzer with impressive energy saving.

GRAPHICAL ABSTRACT



Introduction

Experts suggest that “the near-permanent contamination of the natural environment with plastic waste is a growing concern” [1, p.1]. Estimates show that by 2015, 6300 Mt of plastic waste was generated globally, about 9% recycled, 12% incinerated, and 79% collected in landfills [1]. The annual global production of plastics is expected to reach 1 billion tons in 2050 [2] due to the growing production and extensive demand for plastics. Plastics are made of hydrocarbons with a stable chemical structure, making them resistant to biodegradation and additives containing toxic chemicals that can cause health problems. Thus, many countries enforce regulations to ban or cut down on plastic usage and encourage recycling via incineration or combustion. Studies have shown that the incineration of plastic waste is the primary source of CO₂ emissions. For instance, 850 million metric tons of greenhouse gas emissions were released into the atmosphere from the combustion of plastics in 2019 [3]. Another drawback of incineration is that the produced gas has a limited heating value since complete oxidation releases energy from chemical bonds [4]. When an efficient thermal chemical process is used to recycle plastics into valuable fuels (i.e., H₂) and ensure environmental safety, this tremendous waste can become a considerable low-cost feedstock. It is known that the efficient thermal process of plastic gives a product gas of higher heating value than several fuel types (i.e., paper, textiles, food waste, wood).

Pyrolysis and gasification are thermal processes that have been long considered viable techniques for the sustainable treatment of solid waste with energy recovery options. For instance Ref. [5], reported that plastic pyrolysis could yield 40–50% bio-oil, gas product 35–40%, and 10–20% solid residue. [6], Explained that pyrolysis of mixed plastics produces gas with an average gross calorific value of 38 MJ/kg which is close to that of natural gas (42–55 MJ/kg) and hence can be utilized in various energy-related fields. [7], Studied the degradation of low-density polyethylene (LDPE) under an externally heated fluidized bed reactor using an electrical furnace and analyzed the effect of temperature and the gas residence time on pyrolysis gas composition. Their results validated the findings of [8] that pyrolysis of LDPE around 654 °C yields 19.2 wt.% of gas product. At the same time, the gasification of plastic is thought to have an H₂ conversion efficiency of around 60% [9]. This agrees with [10] who stated that plastic polymer could be converted into H₂ at 60–70% efficiency. [11] evaluated the evolution of H₂ flow rates in pyrolysis and gasification of polystyrene at 700–900 °C, and concluded that for the sake of higher yield of H₂, these two processes are only helpful when the process temperature is above 800 °C.

Gasification differs from pyrolysis because it requires a controlled supply of oxygen, operates at a relatively high temperature of around 1000 °C, and mainly produces gas products containing a low concentration of contaminants (e.g., tar and dioxin). For instance Ref. [12], reported that total tar could be reduced by 44% in steam gasification under a fluidized-bed reactor at 840 °C. Moreover, the conversion efficiency of gasification is estimated at around 80%, which is higher than pyrolysis. While pyrolysis is an irreversible chemical change

caused by heat in an oxygen-free environment at a relatively low temperature of 300–700 °C, producing liquid, gas, and solid residue. However, pyrolysis gas contains a high fraction of contaminants. Ref [13], Discovered that tar yield in pyrolysis of plastics can reach 83.5 wt%. Because it operates in an oxygen-deprived environment at a relatively low temperature, pyrolysis reduces nitrogen oxide and sulfur oxide formation.

Besides, plasma gasification has emerged recently and appears to have potential benefits whereby different operators consider replacing their conventional gasifiers with plasma-fired reactors. Plasma gasification is a particular type of gasification that relies on a plasma torch. This powerful method can induce a temperature above 2000 °C and complete molecular bond dissociation of various solid materials. It implies that feedstock material can be broken down to the atomic level, allowing further complete extraction of fuel from the feedstock in contrast to partial dissociation for lower temperature standard gasification methods. Likewise, the toxic molecules that evolve along with the crude syngas mixture are cracked down by plasma, making the product gas clean and suitable for electricity generation, pure hydrogen synthesis, etc. The plasma conversion of organic matter to syngas can reach 99%, and it has been found that product gas contains an amount of H₂, around 15% higher than syngas produced by generic gasification [14].

In line with plasma gasification, a novel hybrid microwave plasma-enhanced gasification used in this study brings forth a revolutionary change in gasification. It addresses two significant problems that hamper the widespread commercial application of pyrolysis and gasification processes, notably inefficient conventional heating and high concentration of contaminants in syngas. The latter is due to the gasification system that operates at a relatively low temperature and mainly involves pyrolysis as a sub-process within a single gasification unit. Hence, favoring the formation of a high fraction of dioxin. The problems caused by low-temperature processes are inextricably linked with inefficiency in tar cracking and dioxin removal. Thus, standard gasification uses a post-combustion technique for gas treatment at the expense of high treatment costs and energy loss. Regarding the source of heat energy required for these processes, for instance, the use of electrical furnaces is still dominant. Yet, high thermal losses induce increased processing time, leading to high electrical power consumption.

Few researchers have tried microwave-assisted pyrolysis to solve the inefficiency of electrical furnaces [15,16]. Microwave-assisted pyrolysis consists of internal heating in which microwave radiations are absorbed by microwave susceptors mixed with material to be treated, thereby producing the heat required for pyrolysis. The major drawback of microwave-assisted pyrolysis is the limitation in heat transfer caused by the formation of hotspots that influence uneven heating [17].

Therefore, this study explored a microwave-heated pyrolyzer with an electrically heated furnace to ease the choice of an ideal heating method. Even though several industrial heating methods exist, as described by Refs. [18,19] an electrical furnace based on resistive heating is the most widely used in pyrolysis and gasification processes. Here, the resistors are embedded in refractory material and oppose the

Table 1 – Comparison of the electrical furnace with microwave-heated pyrolyzer.

Resistive heating (i.e., electric furnace)	Criteria	Microwave heating (i.e., microwave- heated pyrolyzer)
25–35% High heat loss, Electrical energy to thermal energy	Thermal efficiency Heat loss and energy coupling	80% Lower heat loss, electrical energy to microwave radiations & conversion into heat energy
Poor energy saving, high resistance, high heat loss, slow heating lead to high electrical consumption	Electrical power consumption	Rapid heating, saves over 50% than convention heating

flow of current passing through them by creating friction that, over time, turns into heat. They are made of nickel-chromium alloy, which has a high resistance implying a high electrical input power requirement. The heat transfer mechanism shows that heat energy supplied to the system must dissipate within the external walls of the reactor until the temperature

gets higher than that of the internal walls [20]. “this is a slow and inefficient method for transferring energy into the reacting system” [20, p.1] further stated. In line with this [19] also explained that the energy efficiency of electric furnaces ranges 25–35%, as shown in Table 1.

On the other hand, microwave heating can be explained by two principles. First, ionic conduction occurs when free ionic species exist in a substance to be heated (e.g., salt). The dynamism of ionic constituents (bouncing back and forth) in a delimited zone of importance concerning fast oscillations of electric field triggers the instantaneous superheating within the load. It should be noted that ionic conduction happens at lower microwave frequencies. The second principle is dipole rotation, where polar species (e.g., H_2O) face inertia force; thus, the reorientation tendencies of permanent dipole when subjected to a rapid reversal of an electric field result in energy absorbance. Dipole rotation is thought to occur at an estimated frequency of 300 MHz [21]. Energy absorbed by the material due to dielectric loss is expressed in terms of power dissipation, meaning that when the microwave absorption within the material becomes high, the interaction between microwave and material becomes more intensive. Therefore, since heat tends to distribute evenly from inward to outward zones of heated material, “volumetric heating,” the losses are negligible; thus, a higher heating rate can be reached [22] as explained in Fig. 1. Energy efficiency in microwave heating is

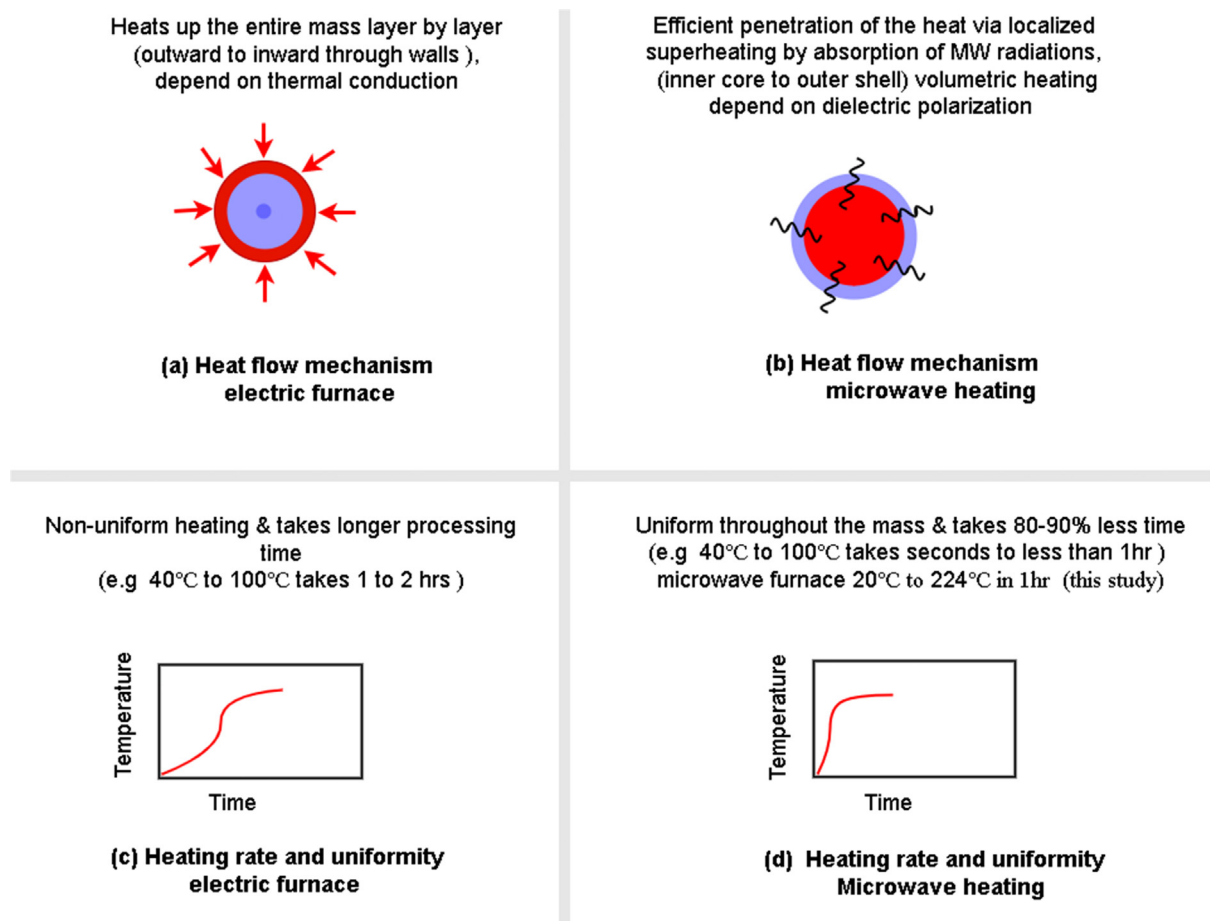


Fig. 1 – Heat transfer in microwave heating versus heat transfer in electric furnace.

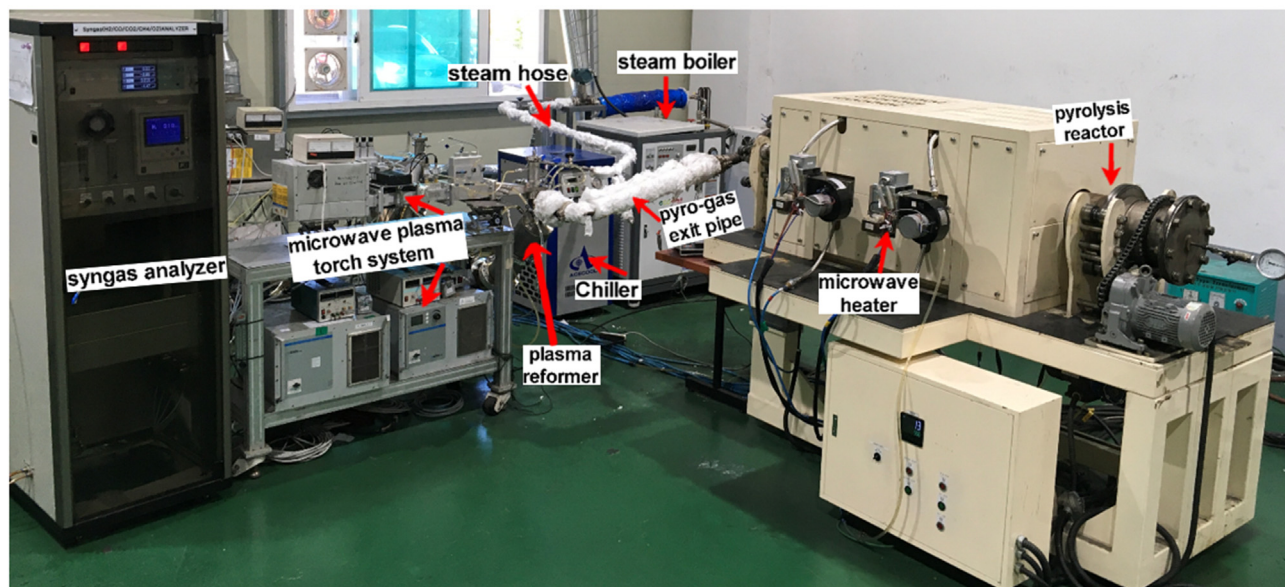


Fig. 2 – Experimental setup of a 100 kg/day HMPEG pilot-scale plant for pure H₂ production.

estimated at 80% [18], as mentioned in Table 1, which further describes resistive heating and microwave heating.

From the energy-efficient plastic waste conversion into H₂ stand point, the mass production of H₂ is twofold; promoting a safer environment and boosting sustainable energy market. Hydrogen (H₂) is currently recognized as a clean energy carrier due to its zero carbon footprints, and high gravimetric energy density (5–13 wt% H₂, 40 gH₂/l, 700 bar) [23,24]. Compared to other fuels, the heating value of H₂ (120 MJ/kg) is 4, 2.8 and 2.4 times higher than that of coal, gasoline, and natural gas (CH₄) respectively [25] and its specific energy density is higher than that of fossil fuels. In terms of electricity, the energy density of hydrogen is 33.6 kWh per kg, higher than that of diesel (12–14 kWh per kg). On top of that, a pressurized tank can be used to store and transport H₂ in a gaseous, liquid or even solid state as a metal hydride [26].

Despite the demand of H₂ in various energy fields, currently ammonia synthesis overtakes other consumers with over 60% of H₂ produced globally [27]. Equally important, the fact that traffic has recently emerged as the first leading field in energy consumption; the release of soot and pollutant emissions, the desirability of H₂ for hydrogen-fueled vehicles is becoming imperative and appears to be a growing trend toward decarbonizing heavy transport and energy demand. For example, to reduce energy consumption in public transport and urban pollution, the United States, Japan, South Korea, Britain, and Germany promoted hydrogen-powered zero-emission vehicles by establishing subsidy strategies like purchase tax cut, and incentives [28].

Although, numerous methods for H₂ synthesis exist, the current investigation on the technical feasibility of commercial-scale production of high-yield H₂ from plastic waste presents a more reliable, safer and robust method for H₂ toward sustainable energy systems. It is known that over 90% of H₂ produced globally comes from commercially established “steam methane reforming and coal gasification [25,27] which

are fossil-fuel sources. Studies have shown that the dependence on fossil fuel not only addresses H₂ fuel needs but also, represents 65% of the global energy demand [25]. With this dominance in mind, the reliance on fossil fuel could trigger an energy crisis as they are nonrenewable sources that are drastically declining, not to mention their substantial contribution to greenhouse gas emissions. Despite, the development and implementation challenges, renewable technologies for hydrogen production including water-splitting processes, a mixture of plastics and biomass (gasification and pyrolysis), supercritical water gasification and others do exist [29–32]. Hence, plastics’ abundance and recyclable nature will help reduce dependence on fossil fuel energy sources. Thus, producing H₂ via clean energy-efficient (HMPEG) technology using plastic waste is an undoubtedly promising way for both economic and environmental safety aspects. This supports the statement of [17] that hydrogen is environmentally friendly when it is produced from renewable sources in a sustainable and efficient process.

Indeed, as mentioned earlier, there have been significant efforts in recent studies on hydrogen production via several methods including pyrolysis and gasification of plastics, though mostly limited to lab-scale. No reported research has successfully applied a hybrid gasification scheme for addressing these problems toward a commercially viable H₂ production process from plastics. Thus, the goal of this research is an experimental feasibility study of a novel method, the “hybrid microwave plasma torch enhanced gasification (HMPEG) process,” that resolves inefficient heating and removes contaminants in syngas for commercial production of high yield and clean H₂. The study is centered around three themes 1) experimental investigation of pyrolysis and gasification characteristics of mixed plastics, 2) evaluation of the performance of HMPEG on syngas composition, tar cracking, and dioxin removal, and 3) examine the heating characteristics of a novel microwave furnace over the electrical furnace.

Table 2 – Proximate and ultimate analysis of different plastics.

Plastic types	Proximate analysis (wt.%)						Ultimate analysis (wt.%)				HHV (MJ/kg)
	Moisture	F.C	Volatiles	Ash	C	H	Cl	N	O	S	
PET	0.61	13.17	86.83	0.0	63.12	4.5	0.0	0.03	0.0	0.05	28.2
HDPE	0.0	0.03	98.57	1.4	85.96	12.03	0.0	0.2	0.0	0.02	40.5
LDPE	0.3	0.0	99.7	0.0	83.0	16.75	0.0	0.0	0.0	0.25	39.5
PP	0.15	1.22	95.08	3.55	85.16	12.47	0.0	0.20	0.0	0.04	40.8
PS	0.25	0.12	99.63	0.0	90.47	9.43	0.0	0.0	0.0	0.08	43.0
PVC	–	9	91	1	38	5	56	0.0	0.0	0.0	19.2

Table 3 – Experimental scheme.

Plastic-type	Quantity (g)	Feedstock ratio (%)	Reaction time(min)	Reaction temperature (°C)
PP/PET/PS	2000	25/50/25	120	500–650
PP/PET	1000	25/75	180	500–650
LDPE/PET/HDPE	3000	25/50/25	120	500–650
LDPE/PET/PP	1500	25/25/50	180	500–650
PS/PET/HDPE	4000	50/25/25	180	500–650
PS/PET/PVC	1000	47/47/6	180	500–650

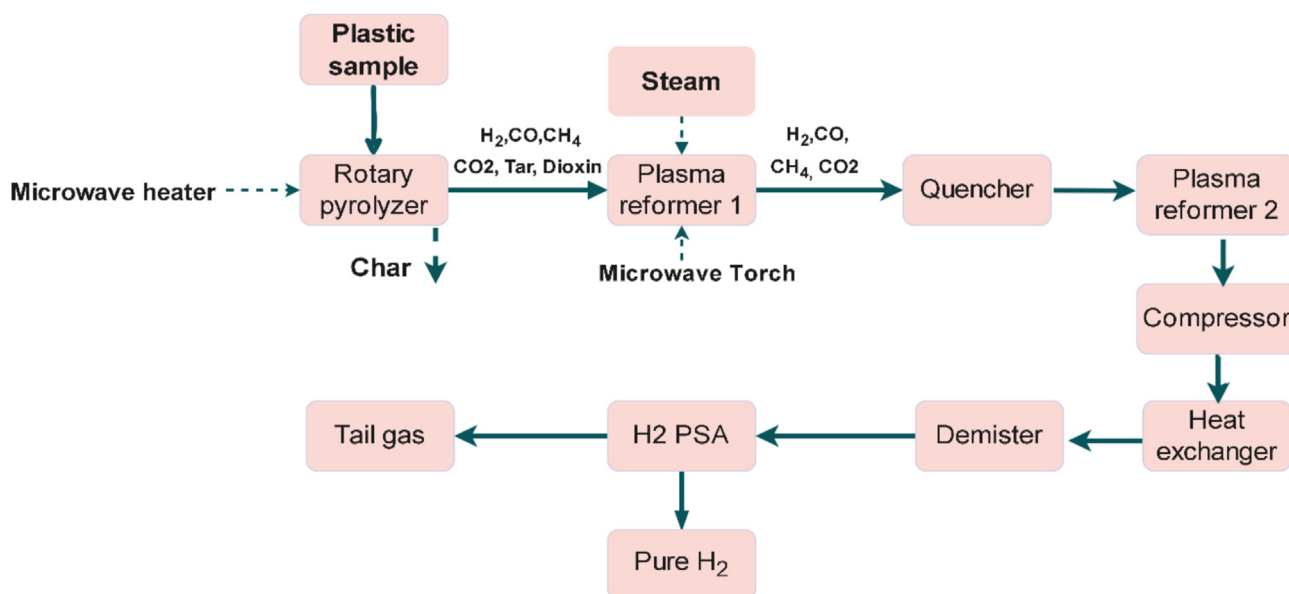
Materials and methods

The mixed plastic waste sample used in this study was collected from household waste and stored in the warehouse of the pilot scale plant HMPEG at 20 °C and 30–50% humidity. As a post-consumer material, it comes in different shapes and sizes. It was mainly composed of low-density polyethylene LDPE(C₂H₄)_n; polypropylene PP (C₃H₆)_n; high-density polyethylene HDPE(C₂H₄)_n; polystyrene PS(C₈H₈)_n; polyvinyl chloride PVC(C₂H₃Cl)_n; and polyethylene terephthalate PET(C₁₀H₈O₄)_n. The chemical and physical characteristics analyses, along with the calorific value of different raw plastic materials, were obtained from Refs. [33–36] as tabulated in Table 2. The plastic samples were fed into the pyrolysis

reactor as received without being shredded into pieces, having an average size of 5 cm in diameter and 30 cm in height and an average density of 934 kg/m³. The proportion of each plastic type in the mixed sample can be found in Table 3.

Description of developed equipment design and process of HMPEG

In this study, the process of converting plastics to H₂ was carried out in two significant steps: pyrolysis, the first stage that thermally decomposes plastics. The resultant crude gas phase product was then supplied to the plasma reformer or the second cracking stage that partially oxidizes this pyrolysis gas with a controlled steam supply under a plasma torch. This led to nearly 100% conversion of organic components to

**Fig. 3 – HMPEG process flow diagram.**

syngas, primarily H_2 , and a minor amount of CO , CH_4 , and CO_2 . Fig. 2 depicts the experimental design of a 100 kg/day pilot plant that comprises HMPEG process equipment such as rotary kiln pyrolysis reactor; microwave heater; pyro-gas exit pipe; steam boiler; steam hose; chiller; plasma reformer; microwave plasma torch system; and gas analyzer. While the process flow diagram presented in Fig. 3 summarizes the stages through which the inlet feedstock is treated till the final target product (H_2). The detailed description is as follows.

Pyrolysis unit and process

A novel rotary kiln reactor (SUS304, $\varnothing 216.3$ mm, and 2.17 m long) of 100 kg/day processing capacity was designed and developed for the pyrolysis of solid fuel. Its main features include improved uniform heat transfer due to vigorous mixing, reduced heat loss, and rapid heating. Upon loading the plastic sample inside the pyrolyzer, the pyrolysis process was initiated by heating the pyrolyzer to the desired reaction temperature of 500–650 °C, which was maintained by controlling the microwave heat input (10.8 kW, 2.45 GHz). Under such supplied heat, a plastic material undergoes a sequence of changes that breaks down a long polymer chain into an unstable low molecular weight monomer. The series of thermal decomposition reactions lead to the final pyrolysis products, notably raw syngas, liquid, and solid residue. The gas mixture from pyrolysis was supplied directly to the steam plasma torch for further gas reforming and pollutant removal. A gas pipe that connects the pyrolyzer to the plasma gasifier was operated above the tar dew point (150–30 °C) to avoid the condensation of hydrocarbon contained in syngas. The temperature rises and pressure change inside the reactor were continuously monitored using a thermocouple (K-type) and pressure gauge. The pyrolysis test runs were batch processes where the solid residue (char) had to be collected, measured, and analyzed after each experiment. However, there was no direct measurement of pyrolysis gas products; instead, syngas composition was analyzed after being reformed under the plasma reformer because these two units (plasma reformer and pyrolysis reactor) are directly connected, as shown in Fig. 2 where the pyro-gas exit pipe connects the pyrolyzer to plasma reformer.

Microwave steam plasma gasification unit and process

This unit has four main parts such as the microwave plasma torch system, plasma reformer, steam supply system, and gas treatment system. The microwave plasma torch system comprises of power supply unit, voltage regulator, magnetron (2.45 GHz), isolator, direction coupler, stub tuner, rectangular tapered waveguide, quartz barrier, quartz holder, and a quartz tube. A plasma torch reformer (gasifier), called a pillar of fire (POF), is a vertically arranged cylinder. Its upper flange connects the quartz tube holder and tapered waveguide. The plasma discharge inside the quartz tube was stabilized by the injection of swirl steam at an optimized flow rate of 3 kg/h. This was maintained by microwave power (7.5 kW, 2.45 GHz) at ambient pressure. The nozzle of the POF permits the syngas from the pyrolysis reactor to be supplied directly to the plasma reaction zone. The nozzles arrangement and gas injection were designed to allow proper gas mixing when impacting plasma. This creates an intense and large volume of

powerful plasma flame (86 mm wide and 900 mm long) with a temperature above 1500 °C capable of reforming raw syngas from pyrolysis and influencing the uniformity of the target product H_2 . The steam supply system consists of a boiler (160 °C, 5 bar), a superheated steam unit, and a hose supplying steam as a gasifying agent. The gas treatment system includes a wet scrubber and quencher (100–200 °C), so hot syngas exiting the downstream plasma reactor must pass through a wet scrubber and quenching system to remove condensable pollutants and impurities and to allow easy gas sampling and measurement. An additional plasma reformer (POF-De-sulfur) was installed as a part of a gas treatment system for removing sulfur-based compounds, etc. Along with the compressor and heat exchanger, other important auxiliary devices include a demister that eliminates moisture in the product gas. At the same time, a pressure swing adsorption unit (PSA) ensures high-purity H_2 recovery by separating impurities from H_2 streams.

Plasma gasification here is a special type of gasification that relies on a microwave plasma torch, a self-sustained energy source device capable of providing the heat energy required for gasification. This eliminates combustion sub-process stages commonly used in standard gasification to sustain gasification reactions. The discharged plasma activates chemical reactions via a transfer of energy of its highly reactive species (ions, electrons, radicals) to the reacting swirl gas. The concentration of free radicals and charge carriers, along with extremely high temperature and density of these plasma species, for instance, reactive O_2 plasma has 3eV and $10^{16} m^{-3}$, respectively [37] give the more greater significant potential for chemical reactivity. A strong electric field continuously energizes these species as they are present in the plasma discharge zone. Thus, this synergic effect enriches gas phase reaction rates in plasma reactors, causing chemical reactions to proceed faster and more efficiently than catalytic-based reactions. It is worth noting that the microwave torch used in this study is an electrode-free device, which, unlike plasma arc, couples microwave power to plasma at an efficiency above 80% through a dielectric window instead of a direct connection to an electrode [38,39].

Experiments and analysis method

Several test runs were performed using a mixed plastic sample at a feeding rate ranging from 1 to 4 kg/h. The experimental scheme is shown in Table 3. The weight of the sample before the test run and the solid residue (char) after each pyrolysis test run were measured using a micro weighing scale balance (CAS model MW-II). The temperature and pressure variation the inside rotary pyrolyzer was controlled using a thermocouple K-type and pressure gauge. The elemental composition and proximate analysis of char from pyrolysis were performed using the ASTM D7582-15 test method (dry basis). The test method used for moisture analysis was ISO 18134-2:2017 while oxygen and fixed carbon were obtained by calculation. A gas sampling pump (N 86 LABOPORT) that connects the syngas exit pipe to the gas analyzer was used. The hot gas exiting the plasma reactor passes through a wet scrubber and quenching system to remove condensable pollutants, impurities and allow easy gas sampling and

measurement. The online syngas sample analysis was done using three different types of gas analyzers: infra-red gas analyzer (model Fe, infrared gas analyzer, Fuji Electric Co. Ltd), Micro-GC (Model G3581A, Agilent Technologies), and Multigas analyzer (model Air well Plus modified, KINSCO Technology Co. Ltd). Micro-GC was used to analyze syngas composition and N_2 , O_2 , and light gaseous hydrocarbon compounds (C_2 – C_4). The gas analyzers incorporate a software package for online data handling. A ball flow meter and digital flow meter were used to control the flow rate of carrier gas. A mass flow meter and a digital monitor were used for superheated steam flow rate control.

Dioxin and furan (PCDD/Fs) sampling

The sampling train was installed at the downstream plasma reformer next to wet scrubber (see Fig. 7 (d)). The dioxin sample collection is a complex system that includes the main sampling train and nozzle as shown in Fig. 7 (d). A typical composition of the whole collection unit operates as follows: suction pipe → cylindrical filter → gas adsorption part (I) of Impinger (3 pcs) → adsorption tube (XAD-2 resin) → gas adsorption part (II) of Impinger (2 pcs) → absorbent (diethylene glycol) → silica gel → pump. The adsorption tube contains standard internal material for sample collection ($^{37}Cl_4$ -2,3,7,8- T_4CDD). The collected sample was then stored at 4 °C or less by blocking the light. The measured sample gas volume 3.06 m^3 collected within 4hrs (experimental duration) and the dilution factor used was 8.

Sample analysis procedure

The analysis flowchart includes three main components: cleaning solution for the suction tube (diethylene glycol solution); XAD-2 resin and cylindrical filter paper. The latter two parts allow purification using $^{13}C_{12}$ -2,3,7,8- T_4CDD and connection to Soxhlet extract in which toluene or dichloromethane is added (16hr duration or more). After liquid extraction, a resultant concentrate of about 1 ml was treated with sulfuric acid until the color fade. After that, it was fed to a multilayer gel column where 150 ml hexane was added. And then it was supplied to an alumina column with 100 ml of n-hexane containing 2% dichloromethane and 150 ml of n-hexane containing 50% dichloromethane. The resultant concentrate of standard internal material for syringe additive ($^{13}C_{12}$ -

1,2,3,4- T_4CDD ; $^{13}C_{12}$ -1,2,3,7,8,9- H_6CDD) gives a final solution of about 20–100 μl . Finally, the selective mass ion measurement, and qualitative and quantitative analysis of the sample were performed using High-Resolution Gas Chromatograph/High-Resolution Mass Spectrometry HRGC/HRMS.

Results and discussion

Syngas composition

The produced syngas was analyzed, and the results are presented in Fig. 4. It can be seen in Fig. 4 (a) that around 70 min of reaction time, syngas volumetric concentration increased sharply from 0 to 70%. Overall, the highest values achieved for H_2 , CO , CH_4 , and CO_2 were (67 vol.%), (7 vol.%), (0.18 vol.%), and (16 vol.%) respectively. A marked increase of H_2 , lower CO , and disappearance of CH_4 may indicate that primary gasification reactions were dominant as favored by suitable reaction conditions under the plasma reformer.

Primarily, water gas shift reaction (WGS): $CO + H_2O \rightleftharpoons CO_2 + H_2$ $\Delta H^0 = -42 kJ/mol$: our results from different test runs showed that when gasification reactions were initiated, values of CO reached 8–14 vol.%, and as the reaction progressed, it decreased rapidly to less than 5 vol.%. In comparison, H_2 concentrations evolved at nearly steady rates above 60 vol.%, as illustrated in Fig. 4(a). This could be due to the high efficiency of the water gas shift reaction that converts CO and H_2O into H_2 and CO_2 . Of the different steam flow rates and plasma power tried, 3 kg/h and 7.5 kW, respectively, showed high sensitivity to higher CO fraction conversion. Note that with optimized power and steam flow, H_2 concentration remained higher than CO regardless of carbon in the system, indicating that a higher amount of reactive OH^- was formed in the plasma reactor. It is believed that WGS reaction under excess steam plays a significant role in increasing H_2 yield. Generally, the reactivity follows a mechanism of gasification reactions, which include hetero and homogenous reactions of H_2O , O_2 , H_2 , and CO_2 with gaseous hydrocarbons, residual carbon, and fly ash commonly known as steam methane reforming; and response for the conversion of solid carbon from low-temperature pyrolysis, etc. The effects of steam gasification reactions have been similarly described by Ref. [40].

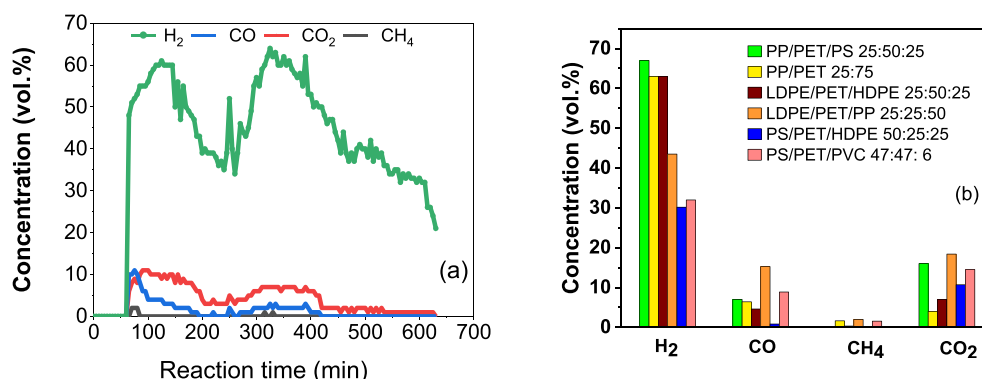


Fig. 4 – Syngas production rate; Fig. 4 (a) Syngas distribution versus reaction time on N_2 -free basis. Fig. 4 (b) Syngas composition according to plastic proportions in selected test runs.

Table 4 – Syngas composition and calculated yield on a weight basis.

Syngas	Concentration (vol%)				Weight (g)			
H ₂	67	63	50	40.7	150.9	127.4	85.2	58
CO	7	4.6	5	2.7	220.8	130.3	119.3	54
CH ₄	0.18	0.32	2	5	3.2	5.1	27.2	57.2
CO ₂	16	7	6	12.6	739.2	311.5	225	396.2

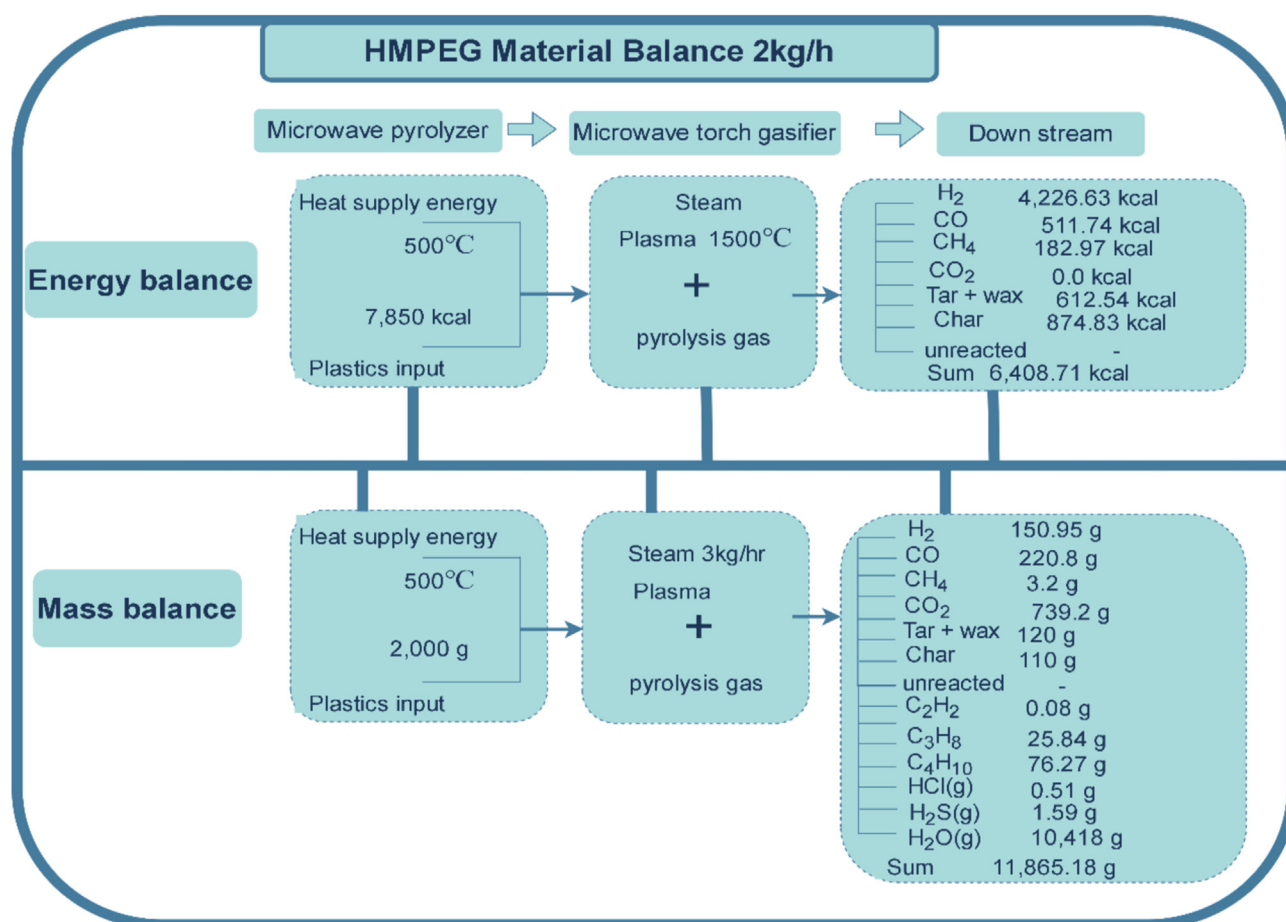
More importantly, a substantial increase in H₂ could be due to the sensitivity of the tar steam reforming reaction to plasma temperature (~1500 °C): $C_mH_n + aH_2O \rightarrow bCO + cH_2 + dC_xH_y$, where C_mH_n denotes tar compound; C_xH_y is a light hydrocarbon while a, b, c, and d represent moles of steam, CO, H₂, and light hydrocarbon, respectively. The effectiveness of tar steam reaction at high temperatures has been confirmed by Ref. [41] who further concluded that tar is converted completely at around 1200 °C while soot decomposes at 1400 °C.

It should be noted that the proportions of plastic types in a mixture shown in Table 3 are part of the factors that determine product distributions, as indicated by their respective properties tabulated in Table 2. Thus, data in Fig. 4 (b) showed rates of syngas formation obtained from treated plastic shares. Generally, the mass fraction of PET >25% seemed to

have a higher increment of H₂ over 5%, compared to other plastics that only gave an average increment of H₂ by 3%. Further quantities of PET can indeed result in an increased production of H₂. This agrees with the findings of [42] who explained that pure PE gives a high amount of gas product. Specifically, Ref [42] obtained a syngas flowrate 21 kmol/h when running the predictive calculations of the gas yield from the gasification of mixed propylene and polyethylene using ASPEN plus. However, for this research, we aimed to use various plastics that directly affect the accumulation of plastic waste.

Tar steam reforming and water gas shift reactions contribute significantly to syngas composition. Particularly, gasification efficiency increased when tar conversion became effective. For instance, at 91.8% tar cracking efficiency, H₂ increased by nearly 30% from 40.7 vol.% to 67 vol.%, as shown in Table 4. In addition to mass balance, the estimated energy balance from the 2 kg/h feed rate is presented in Fig. 5. In some test runs, the CO₂ fraction in syngas reached 16 vol% as shown in Table 4, which could be due to excess steam reforming reactions, as steam is an oxidizer. Hence, as CO decreases, CO₂ increases slightly, but regardless of CO/CO₂ ratio, the H₂ fraction remained over three times higher than CO₂.

The results on a weight basis and volumetric concentration from selected test runs are presented in Table 4. The material balance of a typical experiment is shown in Fig. 5. The

**Fig. 5 – Mass and energy balance of HMPEG process.**

maximum yield of H_2 achieved was 150.9 g/kg/hr., equivalent to 15 wt.% of the initial sample. The weight calculations considered experimental parameters such as reaction time, syngas fractions, and ideal gas molar volume (22.4 l). Also, the N_2 balance in the system was considered, for weight calculations purpose. When the inert gas N_2 (15.7 lpm) was blown into the reactor, and the measured concentration of N_2 in the outlet gas mixture was 79.54 vol%. However, N_2 has a pronounced dilution effect as it seemed to have cut the syngas volumetric concentration by half.

In examining the production rate of H_2 (vol.%) from several test runs, a readiness of our data was observed, specifically, a higher fraction of H_2 in syngas where it remained above 60 vol%. A minor change in concentrations ($\pm 7\%$) was mainly due to the air sneaking inside the pyrolyzer, as it was not perfectly an airtight device. The achieved production efficiency of H_2 (67 vol%) is much higher than commercial steam gasification in fluidized bed H_2 (35–40 vol%) [43].

The current investigation proved that higher production rate of H_2 can be achieved via a compact system at ambient pressure without a catalyst or other costly complex systems. On the contrary, previous findings have indicated that the commercially accepted technique for increasing H_2 concentration only applies catalysts for reforming syngas via gasification [27,44]. For instance Ref. [45], investigated the effect of Ni–Mg–Al catalyst on the yield of H_2 during steam pyro-gasification of plastic waste (HDPE and PTE) in a tubular furnace heated at 600–900 °C. They concluded that the H_2 concentration was around 60 vol% due to a controlled catalyst-plastic ratio (1:2). Similarly, this catalytic ability in H_2 production had been confirmed by Ref. [46] who used several Nickel based catalysts for steam gasification of propylene. Furthermore, an experiment on the pyrolysis of mixed plastics in fluidized bed reactor heated at 600–700 °C was conducted by Ref. [47]. The reduction of the yield of wax product and increase in gas yield was attributed to the complex burnt lime catalyst used as a bed material and steam as fluidizing gas. However, the cost of catalyst, and coke deposition which deactivate the catalyst and prevent the gaseous product from reaching the catalyst thereby affecting the overall process efficiency have been reported as a significant drawback of the catalyst-based processes.

Other related research works on H_2 synthesis from a mixture of biomass and plastic which hold only an H_2 production rate below 50 vol% as have been reported by Refs. [30,31,48]. Specifically, in the experiment by Ref. [44], a feeding blend of 80% biomass (wood sawdust) and 20% propylene was employed for hydrogen production via pyrolysis and gasification. The highest yield of H_2 attained was 36.1 vol%

On the other hand, some researchers proposed a supercritical water gasification as a promising thermal conversion method of hydrogen synthesis since it offers high chemical reactivity at low temperatures and is known as effective for treatment of high moisture content solid waste including biomass and marine plastic waste thereby lowering the pre-treatment cost [49]. Particularly [32], performed supercritical water gasification of polypropylene in quartz tube reactor at 500–800 °C and obtained 79.86 wt% of carbon efficiency and claimed that the gasification efficiency was found to be 10% greater than that of steam gasification [50]. used 100 ml of

biomass samples in supercritical water gasification. The results showed an increase in total gas products from 23.7% to 28.3% while the hydrogen yield varied from 6.6% to 9.4% at temperatures 650 K–700 K. Despite a high-pressure operation (23.2–38.7 MPa), and lower H_2 yield, the researchers also reported that the cost of H_2 produced is much higher than that of H_2 from natural gas reforming (i.e. 2\$/kg H_2) [27].

In addition to the processes discussed above, green technologies for hydrogen production including water splitting methods (electrolysis, thermolysis, photolysis) which split water into H_2 and oxygen (O_2), and many more exist. However, many of these methods are still in the development stage and more time is needed for large-scale production (i.e. photolytic process); while the low H_2 production rate, low efficiency, high capital cost, and corrosive process elements are among the main challenges as discussed by Ref. [29].

Contaminants control in HMPEG gasification

The concentration of tar in syngas

The analyses demonstrated that syngas reforming under plasma torch yields minor traces of hydrocarbons C2 to C4 less than 1%, as shown in Fig. 6. In particular, Fig. 6(b) shows that the C2 to C4 fraction in syngas followed a declining trend while H_2 , CO, CH_4 , and CO_2 took the opposite direction, and for more clarity, Fig. 6(a) illustrates this specific change, for instance, concentrations for C_2H_4 , C_2H_6 , C_3H_8 , and C4 were 0.1%, 0.0%, 0.7%, and 0.49% respectively. This decrease in C2 to C4 hydrocarbons is related to a significant reduction of the concentration of total tar in syngas as it is known that the lower concentration of light gaseous hydrocarbons, the lower the heavy stable tar (polyaromatic hydrocarbon PAH) content in the dry gas [51,52]. Fig. 6(b), present the concentrations of permanents gas and light hydrocarbons (C2–C4). Also, Fig. 6(b) shows the gas composition when N_2 gas was injected in the pyrolyzer. As mentioned earlier, N_2 (15.7 lpm) was used for the mass balance purposes. However, it is clear that the forced injection of a relatively high amount of carrier gas (N_2) into the system has a pronounced dilution effect on H_2 and other syngas concentration as shown in Fig. 6 (b).

For estimating tar concentration, we considered dry tar residue normalized by volume of sampled gas:

$$C_t = \frac{W_t}{V_g} [g/Nm^3]$$

where C_t denotes concentration of tar in syngas [g/Nm³], W_t . Weight of tar (g) measured residue is the volume of sampled gas (Nm³). The tar concentration in dry exhaust gas was estimated at 0.078 g/Nm³ and the tar conversion efficiency stood at 91.8% which was determined by comparing tar content at the inlet of the plasma torch reformer and in the outlet stream. The result complies with the acceptable limit of 0.1 g/Nm³ while for internal combustion (IC) gas engine and gas turbine applications, tar levels less than 50 and 10 mg/Nm³ respectively are required [53], and the reported tar yield in most catalytic steam gasification of plastics range 100–200 g/Nm³ [54]. Generally, it is known that at around 900 °C, oxygenated tarry compounds from low-temperature pyrolysis are converted into aromatic and light PAH compounds. It is followed by the polymerization of light species resulting in

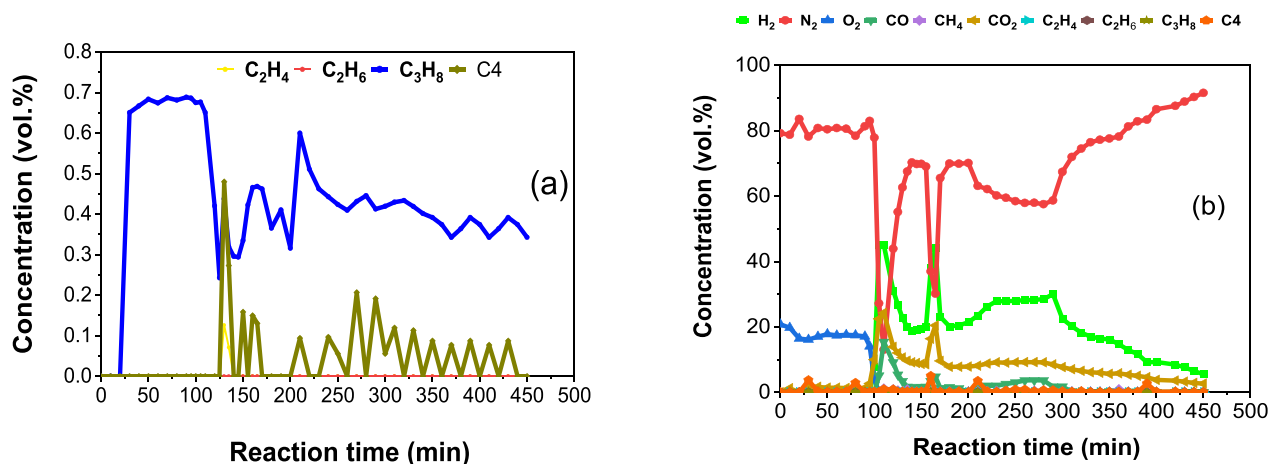


Fig. 6 – Volumetric concentration of permanent gas and light gaseous hydrocarbon (C2–C4). Propane, butane, and other hydrocarbons synthesized by pyrolysis decreased to below 1 vol%.

heavy stable PAH of a small fraction in syngas, and then above 1050 °C only minor traces of stable PAH tar exist [55], meaning that tar compounds yield an undetectable amount that is often ignored. This condition is thought to occur in the reaction zone of the swirl steam plasma torch reformer (900–1500 °C) used in this study, whereby volumetric concentration for C2–C4 detected ranged from 0.01 to 0.7 vol%.

Furthermore, it is known that tar treatment can be performed in two distinct means namely the in-situ technique which removes tar during gasification and post-treatment method which employs catalyst and mechanical methods including cyclones and filters. Although the latter is a commercially established method, however, it is cost-intensive and the tar concentration in the syngas can still be reduced at a limited value [49]. Thus, our findings showed that in situ tar cracking by microwave plasma torch is effective and could reduce the post-gas clean-up cost.

The concentration of dioxin in syngas

The concentration of dioxins and furans in the dry exhaust gas is illustrated in Fig. 7(a) which was measured from the thermal decomposition of a sample containing 0.34 wt% of chlorine (Cl_2). It can be seen that only a minor value of 0.002 [ng-TEQ/Nm³] for a single dioxin compound (OCDD) was detected, while for furan compounds, only 2,3,4,7,8-PeCDF was relatively higher than others, with a peak value of 0.0148[ng-TEQ/Nm³]. Overall, the result showed that dioxin concentration in product gas stands at 0.024 [ng-TEQ/Nm³]. This value represents a sum of all concentrations of 2,3,7,8-TCDD substituted isomers and was over ten times less than the legal limit value of 0.1[ng-TEQ/Nm³] [56]. Examined the concentration of dioxin from plastics at 1200 °C gasifier and concluded that the dioxin level was 0.014–0.59 [ng-TEQ/Nm³]. Besides plasma temperature that disintegrates dioxins, other factors that allowed the achievement of the lower value include rapid heating and heat transfer uniformity in microwave-heated pyrolyzer and the plasma reactor that allows higher quenching rates (>106 K/s) [57]. In addition, low O_2 content downstream limits the formation and regeneration of

dioxin and furan. This in situ dechlorination attribute of plasma reformer is vital since it avoids toxicity in product gas and costly additional gas treatment facility. Besides, Fig. 7 (b) shows that a CO_2 concentration of 1.9% in dry syngas was the highest value. The variations of CO (ppm) and NOx (ppm) concentration are depicted in graph Fig. 7(c). The NOx concentration level in dry exhaust gas stands at 227.23 mg/Nm³. It was calculated based on raw NOx data, normalized with oxygen content in dry gas, using the expression: NOx at 20.9% O_2 = NOx raw data * $\frac{(1-0.209)}{(1-\%O_2)}$.

The value 227.23 mg/Nm³ falls within the acceptable emission limits as the amount of NOx 400 mg/Nm³ has been set as a standard gasification value, so the lower, the better. In general, the sources of NOx are thermal NOx, fuel NOx and NOx from fuel-rich operations. Here, the main contribution of NOx emission level could be fuel NOx and the amount of inert N_2 (15.7 lpm) forced into the system during the measurement. Because it is known that thermal NOx becomes significant above 1927 °C [58] while in the HMPEG system this temperature is at the core plasma flame.

Gasification efficiency

The energy efficiency of the gasification process is commonly evaluated on a cold gas efficiency (CGE) basis, and often, carbon conversion ratio (CCR) and lower heating value (LHV) are also considered [59]. We have used experimental data and sample analysis results to calculate these metrics. Fig. 8 illustrates the results obtained in selected test runs.

$$CGE(\%) = \frac{Y_g * LHV_{syngas}}{m_f * LHV_f + P_{steam} + P_{plasma}} * 100\%$$

where Y_g represents syngas yield; m_f feed mass flow rate, P_{steam} , P_{plasma} denote power used to heat steam and plasma power, respectively.

As shown in Fig. 8 (a), the maximum cold gas efficiency attained was 65.8%, and the lowest was 32%. Several factors may affect gasifier efficiencies, such as low syngas yield, chemical energy loss in tar, and gasifier heat loss which is

generally estimated at 2–5% of supplied energy. The highest conversion of carbon in plastic feed into valuable syngas was found to be 97.4%, as illustrated in Fig. 8(b). This agrees with previous studies that CCE in plasma gasification can reach 92–98% [59]. The highest efficiency (CCE) of 97.4% in our system could be attributed to the reforming power of the plasma torch. Despite greater tar cracking efficiency of 91.8%, the residual carbon in fly ash can also be converted into CO and H₂, thereby making additional gains. The calorific value of producer gas, LHV of 2.8–5.2 MJ/Nm³, was achieved, as shown in Fig. 8(c). However, steam plasma gasification of plastic waste can have an LHV of 7.8–27.2 MJ/Nm³ [60]. The first cause of a relatively low LHV of 2.8–5.2 MJ/Nm³ is the lower amount of CO and CH₄, as shown in Fig. 4 and Table 4. Meanwhile, H₂ has the highest fraction in syngas, around 70 vol%; thus, H₂ alone represents 90% of LHV obtained. The second major cause is the N₂ dilution effect from undesired air blown into the system.

For H_2/CO ratio, Fig. 8(c) shows that a record high value ranging from 6.3 to 7.2 was achieved due to the greater fractional conversion of CO. Meanwhile, Fig. 8(d) shows that the yield on the weight basis of CO is initially higher than that of H_2 , but CO yield rapidly decreases and disappears while H_2 yield increases and remains higher until the end of the reaction. Thus, the WGS reaction which consumes CO, gets

progressively effective and steady under optimized steam plasma. Note that the change in syngas yield shown in Fig. 8(c) does not affect the syngas production rate (vol%). More importantly, in terms of electricity, the estimated throughput from 1 to 4 kg plastic sample processed ranged from 1.9 to 3 kW, as illustrated in Table 5. The conversion was calculated assuming an IC engine efficiency of 36%. Except for conversion technology, other important factors that affect electrical energy conversion efficiency include syngas quality, such as H_2/CO ratio and gas density. Thus, the electricity recovery rate was found to be relatively high. In line with this [61] stated that plasma could convert solid waste into energy at an efficiency of 51%, while conventional methods can only reach 20%.

Heating potential of a novel microwave-heated pyrolyzer

The thermal profile shown in Fig. 9 revealed an increase of 214 °C within 1 h (from 126 °C to 340 °C). This rapid increase in temperature inside the pyrolyzer shows a higher heat transfer rate. As a result, mixed plastics were wholly decomposed. For example, the weight of char varied from 10 to 16 wt% of the initial sample, and a mass conversion efficiency was estimated at 84%–90%. The interesting fact about a novel microwave furnace is that besides its external heating mode, which

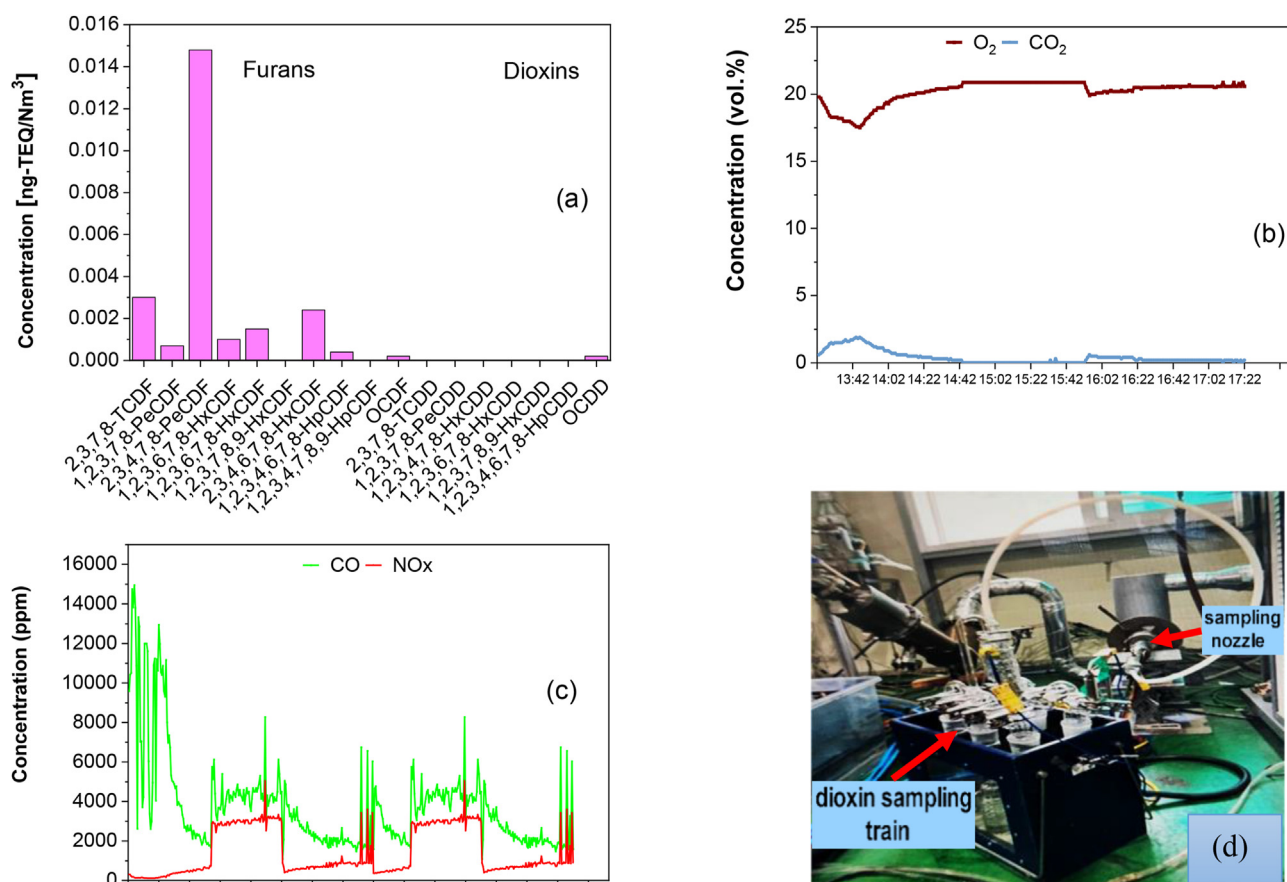


Fig. 7 – Sampling and analysis of emissions in the dry exhaust gas. Fig. 7(a) Distribution of 2,3,7,8-TCDD substituent isomers [ng-TEQ/Nm³] in dry exhaust gas Fig. 7(b) Change in O₂ and CO₂ concentrations in dry exhaust gas; Fig. 7(c) Change in CO and NO_x concentrations in dry exhaust gas; Fig. 7(d) Dioxin sampling train.

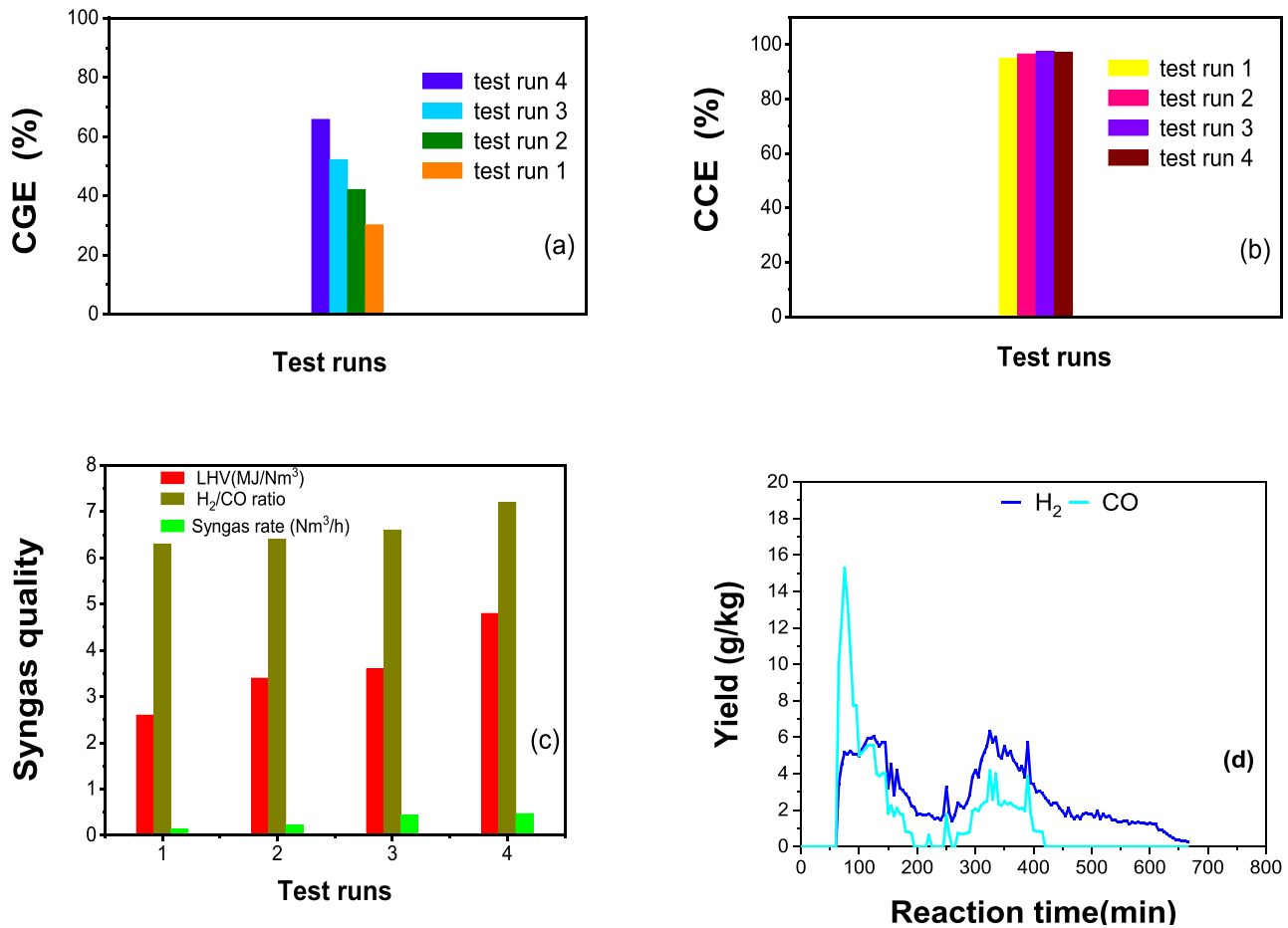


Fig. 8 – Gasification efficiency metrics. Fig.8(a) cold gas efficiency; Fig.8(b) carbon conversion efficiency; Fig.8(c) compiled gasification characteristics (LHV, H₂/CO ratio, syngas yield); Fig.8(d) H₂ yield versus CO yield on weight basis during gasification.

mimics conventional heating, it was found that it takes only 45 min to 1hr pre-heating time to initiate devolatilization reactions.

Energy analysis of microwave-heated pyrolyzer

We calculated the thermal efficiency of microwave-heated pyrolyzer based on energy input, heating profile, and energy consumed during the thermal decomposition of plastics. Fig. 10 summarizes the calculation process and obtained results. For calculation purposes, a sensible heat:

$$Q = m_i \cdot C_{p_i} \cdot \Delta T$$

Table 5 – Syngas to electricity conversion.

LHV (kcal/Nm ³)	Syngas yield (Nm ³)	Electricity (kW)
2088.24	2.25	1.96
2373.84	3.178	3.13
2835.85	2.175	2.55

These performance indicators show that once HMPEG is applied, plastic waste could become a valuable feedstock for energy recovery options.

where m_i is the weight fraction from elemental analysis of the plastic sample, C_{p_i} is the specific heat capacity of each elemental species at 298.15 °C; ΔT denotes temperature difference, and activation energy using a reaction of polyethylene: were considered assuming a conversion efficiency

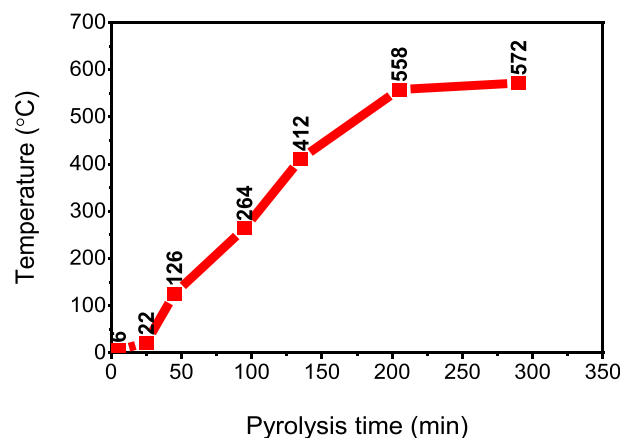


Fig. 9 – Thermal profile inside pyrolyzer under external microwave heating.

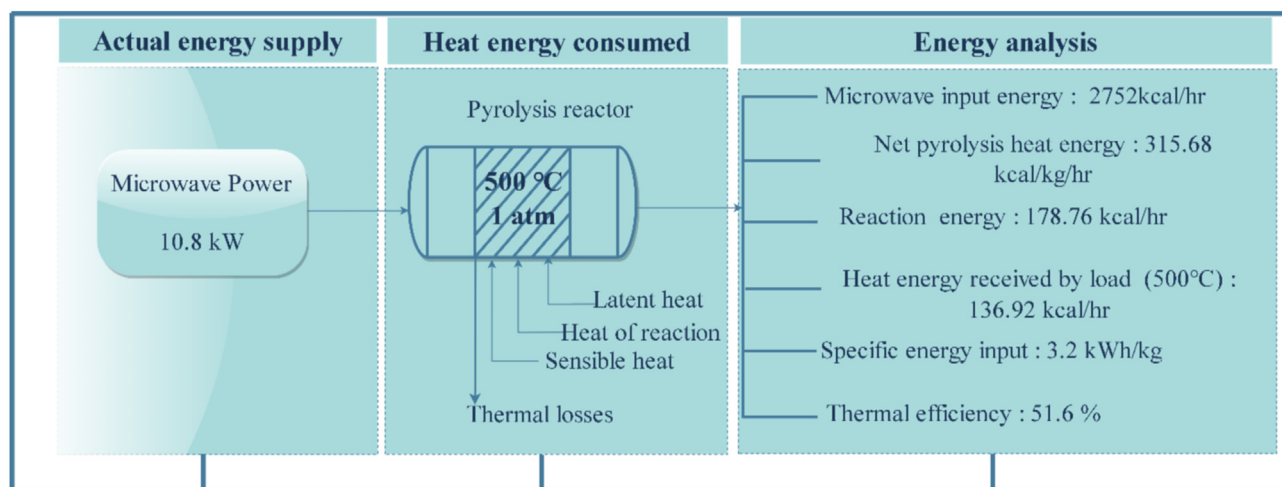


Fig. 10 – Energy analysis. The heating potential of the microwave-heated pyrolyzer.

of 90%, and the enthalpy or latent heat of sublimation of polyethylene 1.84 kcal/mol [62]. Thermal efficiency stands at 51.6% with a specific energy input of 3.2 kWh/kg. Overall, rapid heating, easy control of desired pyrolysis reaction temperature, and vigorous mixing due to the rotary motion of the microwave-heated pyrolyzer influence efficient mass and heat transfer through enhanced solid-solid particle contact, gas-gas and solid-gas particle interactions. This had a significant influence on process outcomes, including pyrolysis product distribution. Particularly avoiding carbon coking and, more importantly, making a better condition to lessen dioxin formation, which is known to be favored in the temperature range of typically 200–300 °C [63].

Furthermore, a novel microwave-heated pyrolyzer was proven capable of processing samples of variable physical properties. This eliminates the need to shred bulk material into smaller pieces, a time-consuming and energy-intensive process commonly found in standard pyrolysis and gasification due to heat transfer limitations. In short, our experimental data validated previous findings that microwave heating exhibits impressive energy saving as rapid heating shortens processing time by 90%, thereby saving electrical power by saving over 50%; thus, its commercial usage could overcome limitations in conventional electric furnaces.

Solid products yield

The measured weight of char residue varied from 10 to 16 wt% of the initial sample and a mass conversion was estimated at 84%–90%. The result of the analysis of char composition from

different test runs is presented in Table 6. This may give an insight into pyrolysis conditions inside the reactor, like gas residence time and heating rate, which affect the mass conversion efficiency. Also, it appears that further char gasification is possible and can help increase syngas energy content, as indicated by a high fraction of fixed carbon of 80–96 wt% and elemental carbon of 88.53 wt%. However, Table 6 also shows that some char residue had high moisture of 50 wt% and low volatile matter (VM) of 0.1 wt%, which means very hard to gasify.

In short, the synergistic characteristic of hybrid gasification also plays a vital role in increased H₂ yield and overall syngas composition. Because improved pyrolysis reaction rates due to microwave heating do not favor carbon coking and promote the formation of a high fraction of gaseous hydrocarbons via depolymerization reactions, these hydrocarbon compounds are characterized by unsaturated chemical bonds that allow them to undergo further reactions via pyrolysis secondary reactions thereby, forming soft polyaromatic compounds like naphthalene, benzene, and toluene. The plasma torch at ~1500 °C decomposes benzene and toluene, other tarry compounds, and permit instant gasification, thereby leaving a nominal rate of formation of stable heavy polyaromatic compounds, which implies high conversion of tar and drastic increase of H₂. Our findings showed that direct plastic conversion into a higher H₂ gas fraction is feasible instead of producing bio-oil as a significant product repeatedly reported in previous studies. Overall, the proposed technology (HMPEG) offers a special flexible operation capable

Table 6 – Analysis of characteristics of char from different test runs.

Proximate analysis (wt.%)					Ultimate analysis (wt.%)						CV(MJ/kg)	
Test runs	F.C	VM	Ash	Moisture	H	C	O	N	S	Cl	HHV	LHV
1	80.7 ^a	18.4	0.9	3.9	3.47	88.53	6.73 ^a	0.22	0.15	—	34.4	32.2
2	19.1	72.3	5.4	3.2								
3	8.1	40.7	0.9	50								
4	99.6	0.1	0.4	0.3								

^a Calculated by the difference.

of processing particles of variable physical properties and decomposing tar, dioxin, and other pollutants while increasing the product's gas energy value. It was found that microwave heating exhibits impressive energy saving as rapid heating shortens processing time by 90%. Thus, commercial use of developed microwave-heated pyrolyzers could overcome limitations in conventional electric furnaces.

Even though we focused on plastics, our method can also treat a much wider variety of solid waste, such as municipal solid waste, sewage sludge, low-grade coal, rice husk, pitch(-asphalt), coffee powder, etc. We conducted several experiments on biomass (wood pellet), low-grade coal, and animal manure. The gas composition showed a similar trend to plastic waste reported in this study. The readiness and repeatability of our data over a long period of operation clearly explain the reliability and robustness of the proposed HMPG technology.

Conclusions

Our data showed that a controlled swirl steam flow rate of 3 kg/h and plasma torch power of 7.5 kW at ambient pressure enriches gas phase reaction rates in the plasma reactor, thereby causing chemical reactions to proceed faster and more efficiently than catalytic-based reactions. Thus, a carbon conversion of 97.4% has been achieved.

One of the significant findings of this study was that the gasification efficiency was enhanced when the plasma torch converted the maximum tar fraction in pyrolysis gas. In particular, the H₂ production rate increased from 40.7 vol% to 67 vol% when a tar cracking efficiency of 91.8% was achieved. This is a significant boost and, to the best of our knowledge, the first of its kind to achieve such efficiency in the production of H₂.

Furthermore, the sensitivity of tar steam reforming reaction to plasma torch temperature of ~1500 °C drives a complete conversion of tar, leaving a negligible fraction of tar in syngas of 0.078 g/Nm³, which indicates a nearly tar-free syngas. Therefore, problems such as fouling, soot deposit, and overall toxicity of tar in the syngas can be avoided. Thus, energy loss and gas treatment costs are minimized.

Another significant finding is that the synergic characteristic of hybrid gasification substantially decreased toxic dioxin to a nominal value of 0.024 ng-TEQ/Nm³. The amount of propane and butane synthesized by pyrolysis decreased to less than 1% while the fraction of H₂, CO, and CH₄ increased to 67 vol%, 7 vol%, and 0.18 vol%, respectively.

A novel rotary microwave-heated pyrolyzer exhibits impressive energy saving and degrades plastics completely without carbon coking thus it was found suitable for pyrolysis. It could be an actual model for expanding commercial microwave pyrolyzers.

Declaration of competing interest

The authors declare that they have no known competing financial interests or personal relationships that could have appeared to influence the work reported in this paper.

Acknowledgments

We acknowledge the financial support from the Ministry of Trade, Industry, and Energy, Republic of Korea (20000495), and Green Science Co., Ltd, located in the Republic of Korea.

REFERENCES

- [1] Geyer R, Jambeck JR, Law KL. Production, use, and fate of all plastics ever made. July; 2017. p. 3–8.
- [2] Qureshi MS, et al. Pyrolysis of plastic waste: opportunities and challenges. *J Anal Appl Pyrolysis* October 2019;152:2020. <https://doi.org/10.1016/j.jaap.2020.104804>.
- [3] Tenhunen-Lunkka A, Rommens T, Vanderreydt I, Mortensen L. *Greenhouse gas emission reduction Potential of European union's circularity related Targets for plastics*, no. 1. Springer International Publishing; 2022.
- [4] Basu P. Biomass gasification and pyrolysis. 2010.
- [5] Matuszewska A, Owczuk M, Biernat K. Current trends in waste plastics' liquefaction into fuel fraction: a review. *Energies* 2022;15(8). <https://doi.org/10.3390/en15082719>.
- [6] López A, De Marco I, Caballero BM, Laresgoiti MF, Adrados A. Dechlorination of fuels in pyrolysis of PVC containing plastic wastes. *Fuel Process Technol* 2011;92(2):253–60. <https://doi.org/10.1016/j.fuproc.2010.05.008>.
- [7] Mastral FJ, Esperanza E, García P, Juste M. Pyrolysis of high-density polyethylene in a fluidised bed reactor. Influence of the temperature and residence time. *J Anal Appl Pyrolysis* 2002;63(1):1–15. [https://doi.org/10.1016/S0165-2370\(01\)00137-1](https://doi.org/10.1016/S0165-2370(01)00137-1).
- [8] Scott DS, Czernik SR, Piskorz J, Radlein DSAG. Fast Pyrolysis of Plastic Wastes 1990;11(6):407–11. <https://doi.org/10.1021/ef00022a013>.
- [9] Wallman PH, Thorsness CB, Winter JD. Hydrogen production from wastes. *Energy* 1998;23(4):271–8. [https://doi.org/10.1016/S0360-5442\(97\)00089-3](https://doi.org/10.1016/S0360-5442(97)00089-3).
- [10] Brems A, Dewil R, Baeyens J, Zhang R. In: *Gasification of plastic waste as waste-to-energy or waste-to-syngas recovery route*, vol. 5; 2013. p. 695–704.
- [11] Ahmed II, Gupta AK. Hydrogen production from polystyrene pyrolysis and gasification: characteristics and kinetics. *Int J Hydrogen Energy* 2009;34(15):6253–64. <https://doi.org/10.1016/j.ijhydene.2009.05.046>.
- [12] Mayerhofer M, Mitsakis P, Meng X, De Jong W, Spliethoff H, Gaderer M. Influence of pressure, temperature and steam on tar and gas in allothermal fluidized bed gasification. *Fuel* 2012;99:204–9. <https://doi.org/10.1016/j.fuel.2012.04.022>.
- [13] Purevsuren B, et al. Pyrolysis of waste polypropylene and characterisation of tar 2009;33:23–33. <https://doi.org/10.1255/ejms.975>. November 2008.
- [14] Pang Y, et al. Plasma-assisted biomass gasification with focus on carbon conversion and reaction kinetics compared to thermal gasification. *Energies* 2018;11(5). <https://doi.org/10.3390/en11051302>.
- [15] Ludlow-Palafax C, Chase HA. Microwave-induced pyrolysis of plastic wastes. *Ind Eng Chem Res* 2001;40(22):4749–56. <https://doi.org/10.1021/ie010202j>.
- [16] Aishwarya KN, Sindhu N. Microwave assisted pyrolysis of plastic waste. *Procedia Technol* 2016;25:990–7. <https://doi.org/10.1016/j.protcy.2016.08.197>. Raerest.
- [17] Arshad H, Sulaiman SA, Hussain Z, Naz Y, Basrawi F. Microwave assisted pyrolysis of plastic waste for production of fuels: a review. *MATEC Web Conf* 2017;131. <https://doi.org/10.1051/mateconf/201713102005>.

- [18] Thirumaran K, Nimbalkar S, Thekdi A, Cresko J. Energy implications of electrotechnologies in industrial process heating. Doe 2007, <http://energy.gov/downloads/doe-public-access-plan>; 2019 [Online]. Available:.
- [19] Frogner K, Andersson M, Cedell T, Siesing L, Jeppsson P, Ståhl JE. Industrial heating using energy efficient induction technology Conference on Manufacturing Systems Total number of authors : induction technology. 44th CIRP Int. Conf. Manuf. Syst. 2011:1–6.
- [20] Hayes B, Hayes BL. Recent advances in microwave- assisted synthesis. *Aldrichim Acta* 2015;37(2):66–76. January 2004.
- [21] Zhang X, Rajagopalan K, Lei H, Ruan R, Sharma BK. An overview of a novel concept in biomass pyrolysis: microwave irradiation. *Sustain Energy Fuels* 2017;1(8):1664–99. <https://doi.org/10.1039/C7SE00254H>.
- [22] Mishra RR, Sharma AK. Microwave-material interaction phenomena: heating mechanisms, challenges and opportunities in material processing. *Compos. Part A Appl Sci Manuf* 2016;81:78–97. <https://doi.org/10.1016/j.compositesa.2015.10.035>.
- [23] Nabgan W, Nabgan B, Amran T, Abdullah T. ScienceDirect Conversion of polyethylene terephthalate plastic waste and phenol steam reforming to hydrogen and valuable liquid fuel : synthesis effect of Ni e Co/ZrO 2 nanostructured catalysts. *Int J Hydrogen Energy* 2019. <https://doi.org/10.1016/j.ijhydene.2019.12.103>. no. xxxx.
- [24] Möller KT, Jensen TR, Akiba E, Li H. Progress in natural science : materials international hydrogen - a sustainable energy carrier. *Prog. Nat. Sci. Mater* 2017;1–7. <https://doi.org/10.1016/j.pnsc.2016.12.014>. October 2016.
- [25] Shadidi B, Najafi G, Yusaf T. A review of hydrogen as a fuel in internal combustion engines. 2021.
- [26] Chi J, Yu H. Water electrolysis based on renewable energy for hydrogen production. *Chin J Catal* 2018;39(3):390–4. [https://doi.org/10.1016/S1872-2067\(17\)62949-8](https://doi.org/10.1016/S1872-2067(17)62949-8).
- [27] Review A. Biofuels production by biomass gasification : a review. 2018. p. 1–31. <https://doi.org/10.3390/en11040811>.
- [28] Chang X, Ma T, Wu R. ScienceDirect Impact of urban development on residents ' public transportation travel energy consumption in China : an analysis of hydrogen fuel cell vehicles alternatives. *Int J Hydrogen Energy* 2018;1–13. <https://doi.org/10.1016/j.ijhydene.2018.09.099>.
- [29] Kumar SS, Himabindu V. Materials science for energy technologies hydrogen production by PEM water electrolysis – a review. *Mater. Sci. Energy Technol.* 2019;2(3):442–54. <https://doi.org/10.1016/j.mset.2019.03.002>.
- [30] Unless R, Act P, Rose W, If T, Rose W. Hydrogen production from biomass and plastic mixtures by pyrolysis-gasification. 2014.
- [31] Alipour R, Al A, Melati M. In: Hydrogen production from mixture of biomass and polyethylene waste in fluidized bed catalytic steam Co-gasification process, vol. 35; 2013. p. 565–70. <https://doi.org/10.3303/CET1335094>.
- [32] Bai B, Wang W, Jin H. Experimental study on gasification performance of polypropylene (PP) plastics in supercritical water. *Energy*; 2019, 116527. <https://doi.org/10.1016/j.energy.2019.116527>.
- [33] Anuar Sharuddin SD, Abnisa F, Wan Daud WMA, Aroua MK. A review on pyrolysis of plastic wastes. *Energy Convers Manag* 2016;115:308–26. <https://doi.org/10.1016/j.enconman.2016.02.037>.
- [34] Surenderan L, Saad J, Zhou H, Neshaeimoghaddam H, Rahman AA. Characterization studies on waste plastics as a feedstock for energy recovery in Malaysia, vol. 7; 2018. p. 534–7.
- [35] Dubdub I, Al-Yaari M. Pyrolysis of mixed plastic waste: I. kinetic study. *Materials* 2020;13(21):1–15. <https://doi.org/10.3390/ma13214912>.
- [36] Shemwell BE, Levendis YA. Particulates generated from combustion of polymers (plastics). *J Air Waste Manag Assoc* 2000;50(1):94–102. <https://doi.org/10.1080/10473289.2000.10463994>.
- [37] Primc G. Generation of neutral chemically reactive species in low-pressure plasma. *Front Physiol* 2022;10(May):1–8. <https://doi.org/10.3389/fphys.2022.895264>.
- [38] Bogaerts A, Neyts E, Gijbels R, Van der Mullen J. Gas discharge plasmas and their applications. *Spectrochim Acta Part B At Spectrosc* 2002;57(4):609–58. [https://doi.org/10.1016/S0584-8547\(01\)00406-2](https://doi.org/10.1016/S0584-8547(01)00406-2).
- [39] Uhm HS, Hong YC, Shin DH. A microwave plasma torch and its applications. *Plasma Sources Sci Technol* 2006;15(2). <https://doi.org/10.1088/0963-0252/15/2/S04>.
- [40] Kumar M, Kumar S, Singh SK. Plasma technology as waste to energy: a review. *Int J Adv Res* 2020;8(12):464–73. <https://doi.org/10.21474/ijar01/12171>.
- [41] Schraut A, Emig G, Sockel HG. Composition and structure of active coke in the oxydehydrogenation of ethylbenzene. *Appl Catal* 1987;29(2):311–26. [https://doi.org/10.1016/S0166-9834\(00\)82901-2](https://doi.org/10.1016/S0166-9834(00)82901-2).
- [42] Saebea D, Ruengrit P, Arpornwicheanop A. ScienceDirect Gasification of plastic waste for synthesis gas production. *Energy Rep* 2020;6:202–7. <https://doi.org/10.1016/j.egy.2019.08.043>.
- [43] Waldheim L. IEA BIOENERGY, and WALDHEIM CONSULTING. Gasification of waste for energy carriers. Task 33. A review. 2018:80–1.
- [44] Alvarez J, et al. ScienceDirect Hydrogen production from biomass and plastic mixtures by pyrolysis-gasification. *Int J Hydrogen Energy* 2014;1. <https://doi.org/10.1016/j.ijhydene.2014.04.189>. –9.
- [45] Wu C, Williams PT. Pyrolysis – gasification of post-consumer municipal solid plastic waste for hydrogen production. *Int J Hydrogen Energy* 2010;35(3):949–57. <https://doi.org/10.1016/j.ijhydene.2009.11.045>.
- [46] Wu C, Williams PT. Applied Catalysis B : environmental Hydrogen production by steam gasification of polypropylene with various nickel catalysts, vol. 87; 2009. p. 152–61. <https://doi.org/10.1016/j.apcatb.2008.09.003>.
- [47] Grause G, Matsumoto S, Kameda T, Yoshioka T. Pyrolysis of mixed plastics in a fluidized bed of hard burnt lime. *Ind Eng Chem Res* 2011;50(9):5459–66. <https://doi.org/10.1021/ie102412h>.
- [48] K. Lee, Y. Jing, Y. Wang, and N. Yan, “A unified view on catalytic conversion of biomass and waste plastics,” doi: 10.1038/s41570-022-00411-8.
- [49] Ciu B, Chiaramonti D, Rizzo AM, Frediani M, Rosi L. applied sciences A Critical review of SCWG in the context of available gasification technologies for plastic waste. 2020.
- [50] Demirbaş A. Hydrogen production from biomass via supercritical water extraction hydrogen production from biomass via, vol. 8312; 2016. <https://doi.org/10.1080/00908310490449379>. June.
- [51] Dufour A, Masson E, Girods P, Rogaume Y, Zoulalian A. Evolution of aromatic tar composition in relation to methane and ethylene from biomass pyrolysis-gasification. *Energy Fuel* 2011;25(9):4182–9. <https://doi.org/10.1021/ef200846g>.
- [52] Brage C, Yu Q, Chen G, Sjöström K. Tar evolution profiles obtained from gasification of biomass and coal. *Biomass Bioenergy* 2000;18(1):87–91. [https://doi.org/10.1016/S0961-9534\(99\)00069-0](https://doi.org/10.1016/S0961-9534(99)00069-0).
- [53] Huang J, Schmidt KG, Bian Z. Removal and conversion of tar in Syngas from woody biomass gasification for power utilization using catalytic Hydrocracking. *Energies* 2011;4(8):1163–77. <https://doi.org/10.3390/en4081163>.
- [54] Lopez G, Artetxe M, Amutio M, Alvarez J, Bilbao J, Olazar M. Recent advances in the gasification of waste plastics . A

- critical overview. *Renew Sustain Energy Rev* 2018;82:576–96. <https://doi.org/10.1016/j.rser.2017.09.032>. May 2017.
- [55] Zhang Z, Pang S. Experimental investigation of biomass devolatilization in steam gasification in a dual fluidised bed gasifier. *Fuel* 2017;188(August):628–35. <https://doi.org/10.1016/j.fuel.2016.10.074>.
- [56] Safavi A, Richter C, Unnthorsson R. Dioxin Formation in biomass gasification: a review. *Energies* 2022;15(3). <https://doi.org/10.3390/en15030700>.
- [57] Gomez E, Rani DA, Cheeseman CR, Deegan D, Wise M, Boccaccini AR. Thermal plasma technology for the treatment of wastes: a critical review. *J Hazard Mater* 2009;161(2–3):614–26. <https://doi.org/10.1016/j.jhazmat.2008.04.017>.
- [58] Sethuraman S, Van Huynh C, Kong SC. Producer gas composition and NO_x emissions from a pilot-scale biomass gasification and combustion system using feedstock with controlled nitrogen content. *Energy Fuel* 2011;25(2):813–22. <https://doi.org/10.1021/ef101352j>.
- [59] Ray R, Taylor R, Chapman C. The deployment of an advanced gasification technology in the treatment of household and other waste streams. *Process Saf Environ Protect* 2012;90(3):213–20. <https://doi.org/10.1016/j.psep.2011.06.013>.
- [60] Weiland F, Lundin L, Celebi M, van der Vlist K, Moradian F. Aspects of chemical recycling of complex plastic waste via the gasification route. *Waste Manag* 2021;126:65–77. <https://doi.org/10.1016/j.wasman.2021.02.054>.
- [61] Oliveira M, Ramos A, Ismail TM, Monteiro E, Rouboa A. A review on plasma gasification of solid residues: recent advances and developments. *Energies* 2022;15(4):1–21. <https://doi.org/10.3390/en15041475>.
- [62] Billmeyer FW. Lattice energy of crystalline polyethylene. *J Appl Phys* 1957;28(10):1114–8. <https://doi.org/10.1063/1.1722589>.
- [63] Masoumeh Safavi S, Richter C, Unnthorsson R. Dioxin and furan emissions from gasification. *Gasif.* [Working Title]; 2021. <https://doi.org/10.5772/intechopen.95475>.